21. S. Kacenjar, L. M. Goldman, A. Entenberg, and S. Skupsky, *J. Appl. Phys.* **56**, 2027 (1984).

22. S. Skupsky and S. Kacenjar, *J. Appl. Phys.* **52**, 2608 (1981).

23. E. M. Campbell, W. M. Ploeger, P. H. Lee, and S. M. Lane, *Appl. Phys. Lett.* **36**, 965 (1980).

1.B Effect of Barrier Layers on Burn-Through Time in Parylene

Burn-through experiments have the potential of providing a measure of the quality of laser illumination uniformity. In these experiments, the laser irradiates a spherical target consisting of an inner substrate shell, sometimes covered with a thin signature layer of a moderate-Z material such as Al, coated with a parylene (CH) layer of varying thickness. Nonuniformities in the laser illumination result in different burn-through times through the CH layer; in particular, the shortest burn-through time can be associated with the highest intensities present at the target surface. This effect was first observed in transport experiments carried out on the OMEGA laser system,[1] in which the burn-through time through a layer of CH overcoating a glass sphere was measured using the time-resolved spectrometer SPEAXS.[2] The results could only be modeled by assuming that a small fraction of the laser energy ($<10\%$) was present at two to three times the nominal laser irradiance (I_0, defined as the laser power divided by the target surface area). It was supposed that small hot spots (<20 μm) were responsible for the large burn-through rates. Subsequent modeling of the laser far-field distribution has shown that small phase errors present in the beam before the focusing lens produced such hot spots.[3] Thus, while burn-through experiments cannot provide a full measure of the illumination uniformity, they can indicate the presence and the approximate magnitude of hot spots in the illumination pattern at the target surface.

Qualitative conclusions on the maximum intensity of the hot spots depend on the assumption that no other processes exist that can lead to fast burn-through signals. This assumption was questioned in further experiments that were carried out, after modifications to the laser system, to study the effect of barrier layers on the penetration of hot spots. Barrier layers are thin (<0.1-μm) layers of medium- to high-Z material coated on the outside of the target. The burn-through rates measured in these experiments were faster than those measured in previous experiments;[4] almost ten times the nominal irradiance was required to replicate the measured burn-through rates in bare (uncoated) CH. On the other hand, the addition of a thin Al barrier layer (0.1 μm) resulted in a burn-through rate similar to those observed previously. Figure 35.10 illustrates the results: the ablated areal density was obtained from targets with increasing thicknesses of CH. The ablated areal density for the bare CH increases very sharply and shows no sign of flattening like the simulation curves.

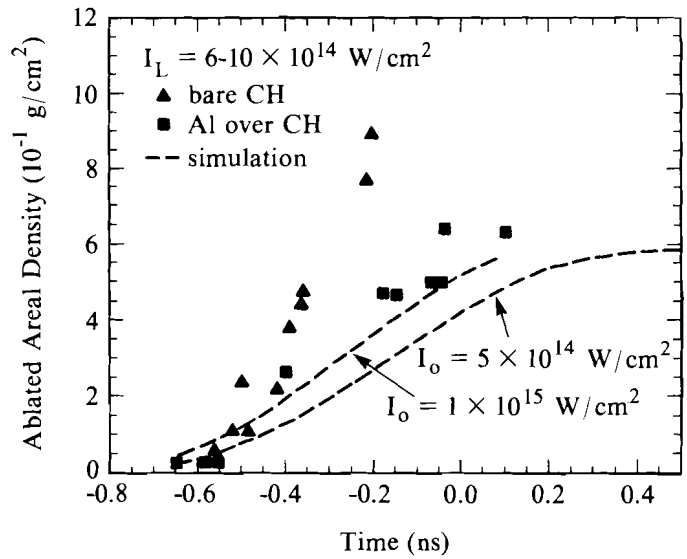

TC2230

Fig. 35.10
Comparison of the burn-through times for CH layers of varying thickness, with and without an Al barrier layer, for the experiment that prompted the study of the effect of various barrier layers on the burn-through time.

It was difficult, at this point, to attribute these large burn-through rates solely to hot spots with intensity larger than ten times the nominal intensity profiles. Several other processes were then proposed to explain the cause of this large burn-through and the effect of adding an outer layer of Al. The processes considered were (1) hot spots of intensities exceeding ten times nominal; (2) shine-through of the laser light early in the pulse while CH is still transparent; (3) a prepulse that would ablate part of the bare CH layer; and (4) filamentation and self-focusing of the hot spots.

These processes are discussed below. Several of them can be eliminated based on the requirement that the addition of a thin Al barrier layer strongly affects the burn-through time. Others required further experiments, which will be described after the discussion of the processes.

Two effects can result from the presence of hot spots: an enhanced penetration of the heat front, and hole drilling, which brings laser-heated material in contact with colder surrounding material, including the signature-layer material (see Fig. 35.11). Simulations of the burn-through experiment using the one-dimensional code *LILAC* indicate that hole drilling does not lead to earlier burn-through than the enhanced penetration of the heat front. There are two difficulties with using hot spots as an explanation for the observed burn-through rates: x-ray and equivalent-target-plane imaging do not show the presence of hot spots with intensities ten times nominal, and one-dimensional hydro simulations indicate that, because the laser burns through a 0.1-μm layer of Al about 700 ps before the peak of the pulse, such a

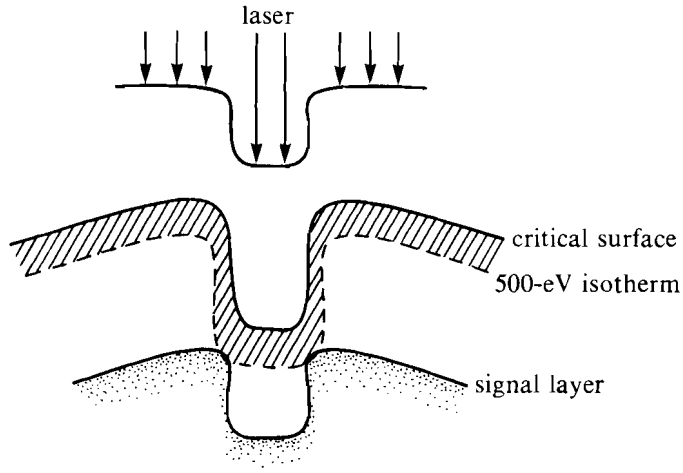

Fig.35.11
Schematic description of hot-spot drilling. A hot spot in the laser beam can effectively drill a hole in the plastic because of the lack of smoothing for 350-nm laser illumination. X-ray emission from the barrier layer can occur when the edge of the heat front around the hole reaches the signal layer.

layer cannot be expected to smooth out the hot spots. Simulations also indicate that a thin barrier layer does not affect hole drilling.

The second process considered, shine-through, assumes that because CH is transparent to UV light at room temperature laser light would penetrate to the signal layer early in the pulse and heat it. This process is very attractive because it would directly explain the effect of adding a thin barrier layer of aluminum. Shine-through was studied using *LILAC*. In the cold target, the laser light was deposited at the boundary of the CH and signal layers. As the electron temperature increased from thermal conduction, in the region immediately in front of the deposition region, the CH became ionized and a critical surface was created: the laser light was then deposited in the zone where the electron temperature reached 1 eV (varying this threshold temperature made little difference). This caused an ionization wave to propagate quickly from the signal layer to the target surface. At that point, the CH layer was a slowly expanding plasma with temperatures of a few electron volts and a density slightly below solid. As the laser energy increased in time, an ablation surface was quickly established and the plastic layer was recompressed to conditions very near those obtained in the absence of shine-through. As a result, burn-through times were not affected by shine-through. Another possible effect of shine-through is that a nonuniform energy deposition at the CH-signal-layer interface may lead to a nonuniform low-density plasma in the CH layer by the time the ablation surface is established. These conditions may seed the Rayleigh-Taylor instability during the recompression, which may lead to mixing of signal layer material into the CH layer. This process is being studied with the two-dimensional hydrocode *ORCHID*.

The presence of a laser prepulse is also an attractive explanation because the burn-through rates increased after changing the oscillator

and removing the prepulse suppressor in the OMEGA laser system. A prepulse absorbed on or close to the surface of the target would have the effect of removing target material before the arrival of the main pulse. As such, the presence of a 0.1-μm Al barrier layer should not make any difference. Also, it can be estimated from Fig. 35.10 that about 4 μm of CH would have to be ablated off by the prepulse to bring the 8-μm burn-through time for the bare CH target in line with the time for the Al-coated target. Ablating 4 μm of plastic requires about 600 J of energy, which is far more than can be delivered by a prepulse. On the other hand, combining a prepulse with shine-through can, in theory, lead to an early burn-through signal. A prepulse could be generated 7 ns before the main pulse if the previous pulse in the oscillator were not suppressed properly. When such a prepulse is deposited at the signature and CH-layers interface, it causes the plastic layer to expand slowly until the main pulse arrives. At that point, the plastic directly in front of the interface has decompressed to densities a few percent of solid. As the main laser pulse establishes a strong ablation front, it sends a shock that recompresses that material. The recompression can heat the CH and a thin layer of the signal layer next to the interface up to 200 eV, which is enough to produce the observed early onset of the x-ray emission. A prepulse energy in excess of 100 mJ is required to produce the needed x-ray emission. Subsequent monitoring by the laser group has established that, if a 7-ns prepulse existed, its energy would be <1 mJ. Therefore, the existence of a prepulse must be ruled out as a cause of early burn-through.

Finally, filamentation and self-focusing could be responsible for the observed fast burn-through times. Both processes can lead to local laser intensities larger than those applied to the target and therefore to a higher estimate of the maximum intensity in the laser illumination. A distinction is made here between the two processes: filamentation arises from initial small perturbations in the laser illumination and is calculated from a linear perturbation of the light-wave equation; whereas self-focusing involves the entire beam (or a hot spot treated as a beam) and is treated by solving the paraxial equation for a Gaussian beam propagating in a medium. The two processes are, of course, driven by the same mechanism: regions of higher laser intensities give rise to regions of lower electron densities in the plasma into which the laser light is refracted because of the lower index of refraction, creating even higher local intensities. These processes are divided into two types, ponderomotive and thermal, depending on whether the plasma is forced out of the high-intensity region by the ponderomotive force of the laser light, or by the high pressures resulting from high temperatures. Filamentation and self-focusing can occur in the corona at all times, although a minimum-beam radius is usually associated with self-focusing. Even though threshold intensities are quoted in the literature for the onset of filamentation and self-focusing, a better criterion to judge their importance is to compare the filamentation and self-focusing growth lengths with the available plasma scale length, i.e., the two processes need enough plasma to develop and focus the light to high intensities. The growth-length scalings found in the literature are obtained from simple models that assume uniform

plasmas and neglect laser-light absorption and heat conduction. Results are not available from code simulations of thermal filamentation or self-focusing under the experimental conditions that apply here: a subnanosecond laser pulse illuminating a solid plastic pellet. Two-dimensional simulations of ponderomotive effects are practically nonexistent because the steep gradients and very short scale lengths generated in the plasma require an extremely fine resolution and, therefore, too many computational zones.

The growth lengths for ponderomotive and thermal filamentation are given, respectively, as the axial wave number of the fastest-growing mode:[5]

$$k_p = \frac{1}{8}\left(\frac{v_0}{v_{th}}\right)^2 \frac{\omega_{pe}}{k_0 c^2}$$

and

$$k_{th} = \frac{\omega_{pe}}{7.5 k_0 c}\,\frac{v_0}{v_{th}}\,\frac{1}{\lambda_{ei}} \quad ,$$

where v_0 is the quiver velocity, v_{th} the thermal velocity, w_{pe} the plasma frequency, k_0 the laser wavelength, and λ_{ei} the electron-ion collision frequency. Note that the ponderomotive growth length is independent of the Z of the material. For the conditions of interest at the time of the burn-through in the CH layer, $T_e = 1$ keV, $I = 1 \times 10^{14}$ W/cm^2; for $n_c/n_e = 10$, the ponderomotive growth length is about 2 cm and the thermal growth length about 0.16 cm. While estimates of these growth lengths may vary (for example, another estimate[6] yields about 0.1 cm and 600 μm for the ponderomotive and thermal filamentation growth lengths, respectively), the growth lengths exceed by about one or more orders of magnitude the distance between tenth-critical and critical surfaces at burn-through time (see Fig. 35.16, used in a later discussion).

The growth lengths for self-focusing are more difficult to obtain, but a rough estimate of the ponderomotive growth length is available.[7] The ponderomotive self-focusing distance is given by

$$R_p = \sqrt{3}\, r_0 \frac{\omega}{\omega_{pe}} \left(1 - \frac{n_e}{n_c}\right)^{1/2} \frac{v_{th}}{v_0} \quad ,$$

where r_0 is the beam or hot-spot radius, ω the laser frequency, and n_e/n_c the ratio of the electron density to the critical density. For the conditions described above, we get $R_p = 3.5\ r_0$, or, for a 20-μm hot spot , $R_p = 35\ \mu$m. It is therefore possible for hot spots with intensity two or three times nominal to self-focus and to produce intensities ten times nominal. However, it is difficult to imagine how the presence of a 0.1-μm barrier layer of aluminum could affect self-focusing, since such a layer is ablated about 500 to 600 ps before the burn-through time for 6 μm of bare plastic.

With none of the proposed processes able to explain the fast burn-through rate, it was decided to conduct experiments in which the plastic layer was overcoated with barrier layers of varying materials and thicknesses; of particular interest were transparent materials with a Z higher than CH. The targets consisted of thick glass shells covered with a 0.1-μm signal layer of Al, a 6-μm-thick layer of CH, and a barrier layer with materials and thicknesses as listed in Table 35.II. These targets were irradiated by the OMEGA laser system at 351 nm with 600-ps FWHM pulses and an irradiance of 8×10^{14} W/cm^2. The beams were focused tangentially to the targets to provide good overall uniformity and absorption. The burn-through time was measured with SPEAXS from the onset of the signal-layer emission. An absolute timing reference to the incident laser pulse was provided by a separate UV fiducial signal.[8]

Table 35.II
Onset times of the x-ray emission from the signature layer for the various barrier layers and the intensity required in simulations to match the measured burn-through times.

Material	Thickness (μm)	Z	Time (ps)	I_s* / I_o
bare	–	–	−250±20	12±1.7
Al	0.1	13	−25±20	4.2±1.2
KCl	0.1	18	−150±20	–
CsI	0.05	54	0±20	4.1±2.0
Au	0.015	79	125±20	2.1±0.2
Au	0.05	79	350±50	1.5

*I_s is the intensity required in simulations to match the measured burn-through times.

TC2396

The temporal emissions of the Al H-α for the set of targets are shown superposed in Fig. 35.12; the continuum has been subtracted and time is with respect to the peak of the pulse. The burn-through time for the bare CH target (areal density of 6×10^{-4} g/cm^2) is the same as that obtained in Fig. 35.10. With one exception—KCl—as the average Z of the outer layer material is increased from 3.5 (bare CH) to 79, the burn-through time increases; the results are summarized in Table 35.II. Again, for an Al barrier layer, the burn-through time of Fig. 35.10 is recovered. KCl, the exception, has an earlier time than Al, even though the two materials have the same Z and KCl is slightly lighter than Al. Also, increasing the thickness of the Au layer also increases the burn-through time; for 0.05 μm of gold, the burn-through is marginal.

To determine whether the change in burn-through time is due only to the added mass of the barrier layer and energy loss to x-ray radiation in the high-Z layer, simulations were performed with *LILAC*. Included in *LILAC* for these simulations, instead of the tabular local thermal equilibrium (LTE) ionization levels and opacities, is a non-LTE

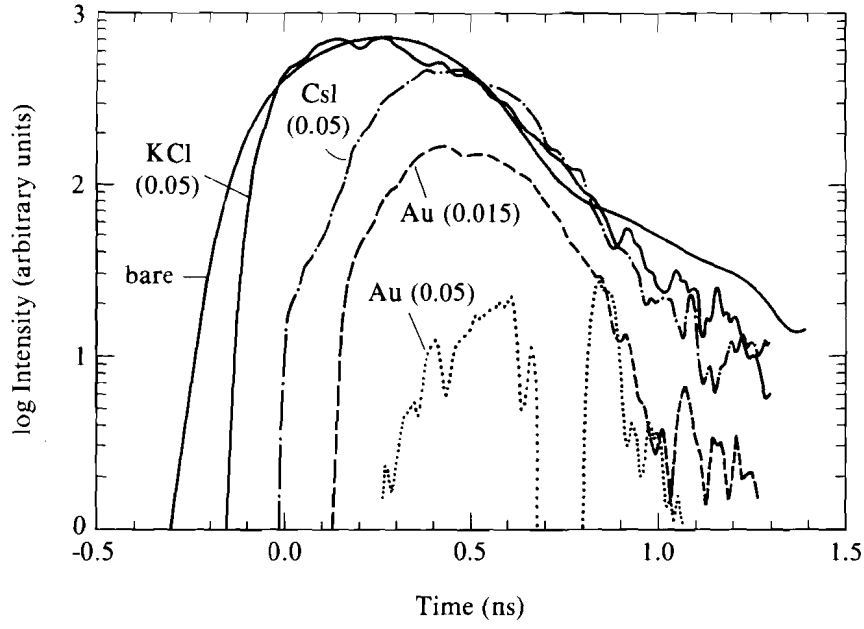

Fig. 35.12
Emission from the signal layer for the various barrier layers. The time is with respect to the laser pulse; the continuum has been subtracted.

average-ion model[9] that provides a better description of the ionization and radiation processes in high-Z material. Each of the cases was first run at nominal intensity, and then at progressively higher intensities until the burn-through time matched the measured time.

The results are shown in Fig. 35.13, where the burn-through time is plotted against the product of the average Z of the material and the areal density of the barrier layer. This scaling is not based on any particular physical basis, but is an attempt to include both the effect of the increasing Z and of the varying density and thicknesses of the barrier layer material. Of interest is that the experimental points for the nontransparent barrier layers, when scaled in this manner, are nearly linear with burn-through time. The burn-through times from simulations, on the other hand, do not show such a dependency on the material within the range of Z and thicknesses used in the experiment (some variations are due to differences in laser intensity in the shots). The burn-through time is slightly longer for Al than for bare CH, CsI, and thin Au. The mass of the CsI layer is about half of the other two. This added mass, and the radiated x-ray energy, should lead to slightly longer burn-through times for these targets than for the bare-CH target. The difference between the Al case and the two others is that the CsI- and Au-coated targets absorb more energy early in the laser pulse than does the Al-coated target, which compensates for the added mass. The longer burn-through time for the thick Au barrier layer is due to the higher mass of that layer and the x-ray radiation losses.

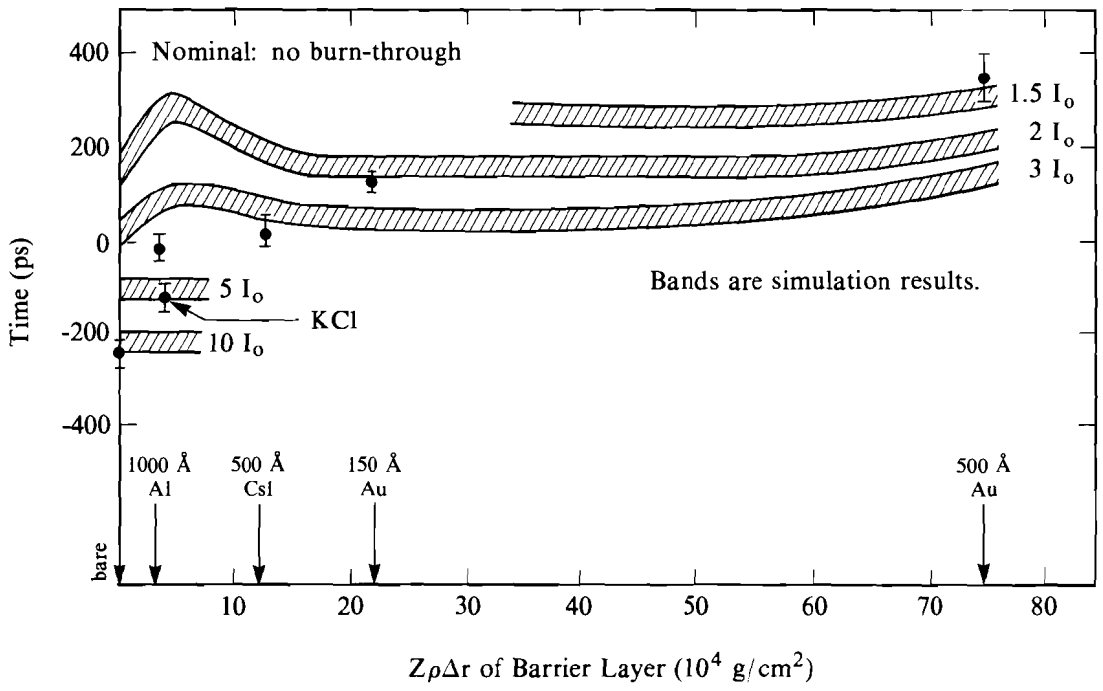

Fig. 35.13
Burn-through time for the barrier-layer targets. The horizontal scaling has no physical significance. The points are the experimental results; the bands are the simulation results at various laser intensities. There is no burn-through in simulations at nominal intensity.

Table 35.II summarizes the experimental results and gives the intensities I_s (normalized to the nominal intensity) that are required in the simulations to match the measured burn-through times. Figure 35.14 shows the scaling of the burn-through time with intensity for the bare target and for the Al and CsI barrier-layer targets. Again, this figure shows how much shorter the measured burn-through time for the bare-CH target is compared to the simulation results; in the simulation, the scaling is similar for all three targets.

The results from this experiment confirm those shown in Fig. 35.10. About ten times nominal intensity is required to obtain the burn-through time for targets without barrier layers and about four times nominal intensity when a barrier layer of Al or CsI is added. The CsI barrier layer is lighter than the Al layer, but it has a higher Z, which seems to lead to a similar behavior. On the other hand, the thin Au layer, which has the same mass as the Al layer but a higher Z than the CsI layer, needs a lower laser intensity to match the experimental burn-through time. Finally, for the thicker Au barrier layer, there is almost agreement at nominal intensity with the experiment. Therefore, both the mass and the average Z seem to affect the processes responsible for the fast burn-through. The KCl barrier layer, which has almost the same mass and Z as Al, does not fit with the others.

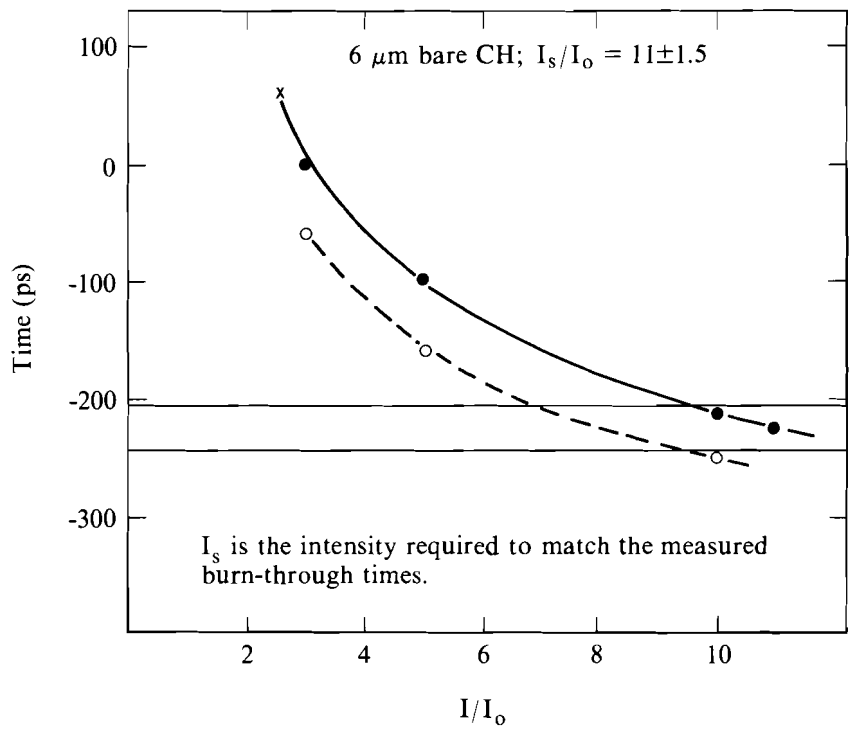

Fig. 35.14
Dependence of the burn-through time on the laser intensity for the bare-CH target and for targets with an Al and CsI barrier layer. The horizontal bands are the experimental times from Fig. 35.12.

The difference between KCl and the other materials is that it is transparent at room temperature (CsI is also transparent at room temperature, but its use as a photocathode material implies that free electrons can be created very quickly by the laser pulse). In a sense, KCl seems to behave partly as CH and partly as an opaque conductor, which indicates that early transparency is still important.

At this point, it appears that this new series of experiments, while providing more data on the problem, has not led to an understanding of the processes that cause the fast burn-through rates through CH. Both the KCl results and the effect of adding a barrier layer of Al on the burn-through time indicate that transparency at room temperature is important. Yet one-dimensional simulations do not show any difference in target behavior due to early shine-through, and measurements have not detected prepulse levels above the expected pulse shape. Another observation is that the thickness and the kind of nontransparent material used in the barrier layer make a difference: thick gold is more effective than thin gold, which in turn is more effective than an equivalent mass of aluminum. This suggests that such processes as self-focusing or radiation smoothing of the hot spots may be present. To appreciate the effectiveness of these processes, conditions in the corona 300 ps before the peak of the pulse are plotted in Fig. 35.15 for four barrier-layer cases at nominal intensity (as a reminder, the observed burn-through in bare CH is −250 ps; in the thin Au, 125

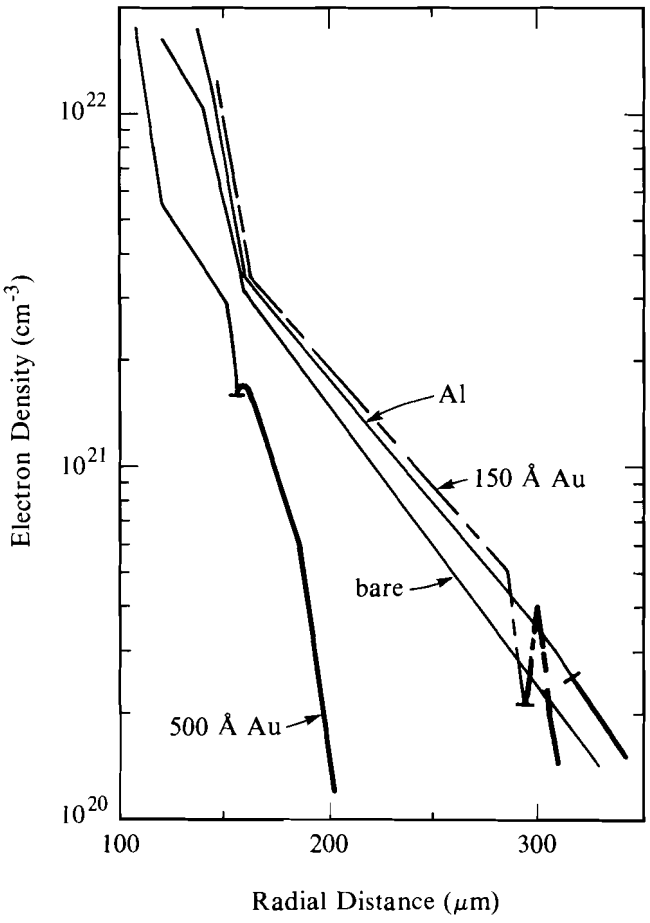

Fig. 35.15
Calculated density profiles in the corona 300 ps before the peak of the pulse for four targets at nominal intensity: bare CH, 0.1 μm of Al, 0.015 μm of Au, and 0.05 μm of Au barrier layers. The thicker part of the profile shows where the barrier-layer material is present. At this time, the nominal laser intensity is 4.7×10^{14} W/cm^2 and the laser intensity at 0.1 critical is 2.0×10^{14} W/cm^2.

ps). At that time, the Al and thin Au barrier layers are far in the blowoff, at densities below 0.01 critical density, where their x-ray radiation efficiency is low; radiation smoothing, therefore, should not be important. The thick Au barrier layer is still present at densities about one-tenth critical density, and it is possible that the Au layer could still radiate enough to smooth out illumination nonuniformities. If radiation smoothing did exist, the effect of the thick Au layer would be to retard the effect of nonuniformity on the burn-through time by keeping the near-critical region smooth for a longer time early in the pulse. The difference between the results for Al and the thin Au layers cannot be similarly explained because both barrier layers are ablated at the same time.

The effectiveness of self-focusing depends on the scale lengths in the corona (ponderomotive self-focusing does not depend on the Z of the material). Figure 35.15 shows that, 300 ps before the peak of the pulse, the scale lengths for bare CH and for the Al and thin Au layers

are almost the same; for the thick Au layer, the scale lengths are shorter than for the other layers because the quarter-critical surface has barely burnt through the Au layer. The distance between the critical surface and the one-tenth critical surface, where self-focusing is more likely to occur, is plotted in Fig. 35.16 as a function of time. As the target outer material changes from CH to aluminum to gold, this distance is shorter early in the pulse, reflecting the steepening of the scale length as the Z of the material increases. But, after the one-tenth critical surface has burnt through the barrier layer, the effect is reversed and the scale lengths are longer for the higher-Z cases. This may be caused by early radiation preheat, which heated the cold CH, creating a somewhat larger mass-ablation rate later in the pulse.

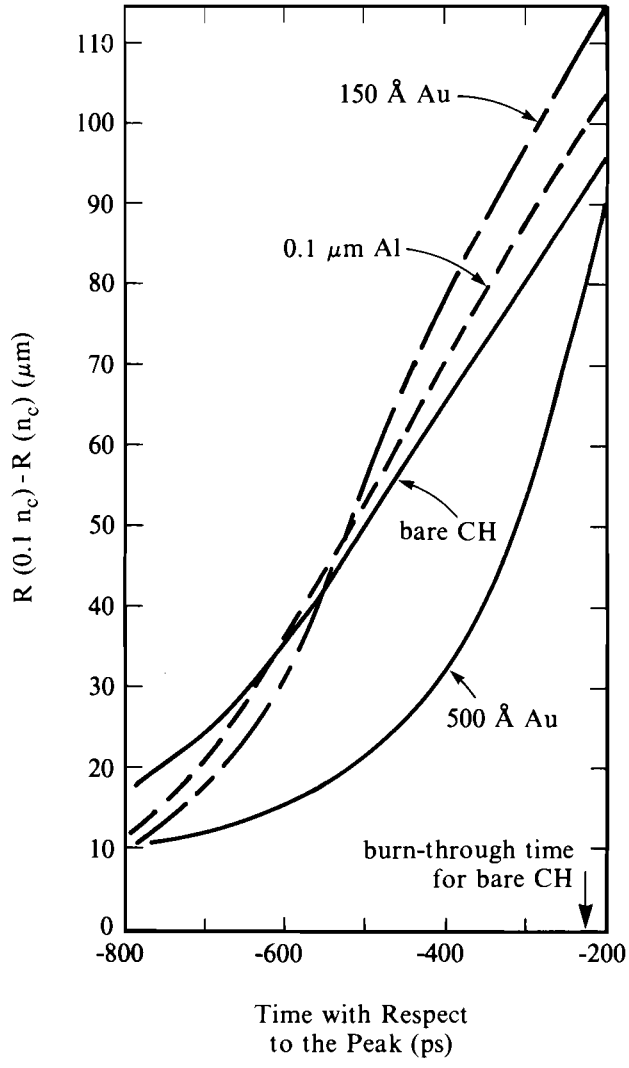

TC2375

Fig. 35.16
Temporal evolution of the distance between the 0.1-critical density surface and the critical density surface for the four targets described in Fig. 35.15. Time is with respect to the peak of the pulse.

Despite these differences, the distances between the two surfaces for CH, Al, and thin Au are the same within less than 10 μm; only in the thick Au case are the distances much shorter. Thus, if self-focusing were occurring, it should be no different for the bare, Al, and thin Au cases; this is especially true since, as early as 300 ps before the peak of the pulse, these layers are below one-tenth critical and should not affect self-focusing between that surface and the critical surface. In fact, because self-focusing grows rapidly (the sound speed is large and the distances involved are of the order of 10 to 50 μm), it is doubtful that self-focusing could even explain the difference in the burn-through time between the thin and thick gold barrier layers.

Summary

In conclusion, experiments with barrier layers consisting of different materials and thicknesses have been carried out in an attempt to understand the processes that cause the large burn-through in CH. The results show that burn-through occurs progressively later during the pulse as the barrier layers change from none, to aluminum, to thin gold, and to thick gold. Simulation results predict that there should be only small differences (< 100 ps) in the burn-through time for all the barrier layers. Several processes, which could lead to fast burn-through rates, were studied: severe hot spots (intensities ten times nominal), shine through, the presence of a prepulse, and filamentation and self-focusing. None of these processes by itself could adequately explain the experimental results because measurements did not show their existence (severe hot spots, prepulse), because they were unaffected by the barrier layers (hot spots, self-focusing), or because one-dimensional simulations showed they had little effect (shine-through). It is very likely that different processes may be responsible for the differences in burn-through time for the various barrier layers: for example, the effect of the aluminum barrier layer and the fast burn-through with a KCl layer support early pulse shine-through; the effect of the thick gold layer gives an indication of early radiation smoothing. Prepulses, filamentation, and self-focusing are the least likely to explain any the observations. The possibility that nonuniform shine-through may cause the layers to become Rayleigh-Taylor unstable is being studied. More experiments are planned to understand the role of each of these processes.

ACKNOWLEDGMENT

This work was supported by the U.S. Department of Energy Office of Inertial Fusion under agreement No. DE-FC08-85DP40200 and by the Laser Fusion Feasibility Project at the Laboratory for Laser Energetics, which has the following sponsors: Empire State Electric Energy Research Corporation, New York State Energy Research and Development Authority, Ontario Hydro, and the University of Rochester. Such support does not imply endorsement of the content by any of the above parties.

REFERENCES

1. P. A. Jaanimagi, J. Delettrez, B. L. Henke, and M. C. Richardson, *Phys Rev. A* **34**, 1322 (1986).
2. B. L. Henke and P. A. Jaanimagi, *Rev. Sci. Instrum.* **54**, 1311 (1983).
3. LLE Review **31**, 106 (1987).